Pis'ma v ZhETF, vol. 93, iss. 9, pp. 575 – 578

The calculation of the Fermi surface with complex topology from norm-conserving cluster perturbation theory for doping dependent electronic structure of the Hubbard model

S. G. Ovchinnikov[+*1)], *S. V. Nikolaev*[∇]

[+]*L.V. Kirensky Institute of Physics SB RAS, 660036 Krasnoyarsk, Russia*

[*]*Siberian Federal University, 660041 Krasnoyarsk, Russia*

[∇]*F.M. Dostoevsky Omsk State University, 644077 Omsk, Russia*

Submitted 24 February 2011
Resubmitted 18 March 2011

In present paper the results of recently developed norm-conserving cluster perturbation theory (NC – CPT) for doping dependent electronic structure of the Hubbard model are reported. We have found that the momentum distribution of the spectral weight strongly depends on the broadening value δ. At the $\delta = 0.1t$ we reproduce the angle-resolved photoemission spectroscopy (ARPES) data, while at $\delta = 0.01t$ we obtain two quantum phase transitions (QPT).

Angle-resolved photoemission spectroscopy (ARPES) provides a lot of valuable experimental data on the electronic structure of cuprates [1]. It was found that Fermi surface has the form of arc around nodal point $(\pi/2, \pi/2)$ with the pseudogap around antinodal points $(\pi, 0)$ and $(0, \pi)$ in the underdoped (UD) region. In the overdoped (OD) region ARPES has found the large Fermi surface around (π, π). The doping of an antiferromagnetic insulator results in a small hole pocket around nodal point which was observed by quantum oscillations measurements [2]. One side of the pocket is the Fermi arc (see discussion of ARPES and oscillations data in the recent review [3]). There is no smooth transformation of the Fermi surface from UD to OD region, it requires two quantum phase transitions (QPT) [4]. Nevertheless, there are no ARPES indications for such transitions. Here we report the results of recently developed norm-conserving cluster perturbation theory (NC – CPT) [5] for doping dependent electronic structure of the Hubbard model. We have found that the momentum distribution of the spectral weight $A(\mathbf{k}, \varepsilon_F)$ strongly depends on the broadening value δ. At the $\delta = 0.1$ (in units of nearest neighbour hopping t) we reproduce the ARPES data, while at $\delta = 0.01$ we obtain two QPT.

The most evident effect of strong electron correlations (SEC) is the "no-double occupancy" constraint that is universal for any SEC system. Specific for cuprates with their quasi-2D magnetic structure is the importance of the spatial spin correlations (short-range magnetic order) induced by large intraplane exchange interaction $J = 2t^2/U$ (U is the Hubbard intra-atomic Coulomb parameter). The neglection of the spatial corrections makes the dynamical mean field theory (DMFT) inapplicable for cuprates. Taking into account both "no-double occupancy" constraint and short-range magnetic order several groups have found the intermediate regime in Fermi surface topology between small pockets in UD and large pocket in OD [6–10]. Different cluster extensions of DMFT [11–15] have also found the importance of the short-range spin correlations for the formation the pseudogap around the antinodal point in hole-doped cuprates. Using the most advanced cellular DMFT plus exact diagonalization (CDFT+ED) method [11] the three type of the Fermi surfaces have been obtained [13] exactly the same as in papers [6–10]. Thus different theoretical approaches result in the existence of the intermediate region in the hole concentration scale p at $p_{c1} < p < p_{c2}$. At $p < p_{c1}$ there are small hole pockets, while at $p > p_{c2}$ the large Fermi surface corresponds to the conventional band theory. The critical values p_{c1} and p_{c2} depend on the model parameters and approximation made. The *ab-initio* calculated parameters of the t-t'-t''-J model result in $p_{c1} = 0.15$ and $p_{c2} = 0.247$.

In the intermediate region the Fermi surface is formed by hole and electron sheets around (π, π) with electron one collapsed at $p \to p_{c2}$ [4, 7]. Up to now there is no experimental evidence for such Fermi surface from ARPES and quantum oscillations measurements. All quantum oscillations studies are restricted to the UD region, presumably due to sample quality [3]. To analyze why ARPES does not see the intermediate Fermi

1)e-mail: sgo@iph.krasn.ru

surface we has study here the hole dispersion and spectral weight $A(\mathbf{k}, \varepsilon_F)$ by NC – CPT method that was used to study undoped Hubbard model recently [5].

Cluster models can be formulated in a general functional framework [16 – 18]. In the initial version [19] the CPT consists of (i) dividing the lattice into identical N-site clusters, (ii) evaluating – by ED – the one-particle Green function $G_0(\omega)$ for cluster with open boundary conditions, and (iii) treating the intercluster hopping t in perturbation theory and recovering the crystal Green function $G(\mathbf{k}, \omega)$. Thus, short-range effects are treated exactly, while long-distance propagation is treated at the single-particle analog.

Usually step (ii) proceeds according to the Lanczos method. In 2x2 cluster for the Hubbard model the number of eigenstates is equal to $4^4 = 256$. The Lanczos method takes into account only the ground and a few excited states ignoring all other. If we write down the exact representation of the electron creation operator at atom f with spin projection σ in terms of the multi-electron eigenstates $|p\rangle$ and $|q\rangle$ of the cluster

$$a^\dagger_{f\sigma} = \sum_{p,q=1}^{256} \langle p|a^\dagger_{f\sigma}|q\rangle |p\rangle\langle q|, \tag{1}$$

then the Fermi anticommutator

$$\{a_{f\sigma}, a^\dagger_{f\sigma}\}_+ = 1 \tag{2}$$

can be treated as the sum rule providing the norm conservation for electron. We want to emphasize that this sum rule is satisfied only when all cluster eigenstates are included in the right side of the Eq. (1). Ignoring excited states results in the violation of the sum rule. In another words some part of electron spectral weight will be lost. Let's introduce the f-factor to measure total spectral weight

$$f = \int d\omega A(\mathbf{k}, \omega). \tag{3}$$

The exact value for $f = 1$ is achieved only when all excited eigenstates are included. Contrary, if one restrict himself only to the lowest in energy multi-electron states with $|n_e = 4, S = 0\rangle$ and $|n_e = 3, S = 1/2\rangle$, $|n_e = 5, S = 1/2\rangle$ (basis for "effective single band Hubbard model") the f-factor is equal to $f = 0.395$. As was shown in recent work [5] it is possible to get $f \approx 0.999$ by taking into account 15–20 excited states. The calculation with controlled f-factor with $1 - f$ less then 1% we call the norm conserving one.

The Hubbard operators $X_i^{pq} = |p\rangle\langle q|$ for the cluster centered at $\mathbf{R}_i$ naturally appear in the right side of Eq. (1). In this representation electron is given by a linear combination of the Hubbard fermions (excitations between $|N_e, S\rangle$ and $|N_e \pm 1, S \pm 1/2\rangle$ configurations). It is convenient to introduce a vector $\alpha = (p, q)$ instead of a pair of final p and initial q states [20]. Each vector α corresponds to some Hubbard fermion if $\gamma_\sigma(\alpha) = \langle p|a^\dagger_{f\sigma}|q\rangle \neq 0$. The main CPT equation [19] for the Fourier transform of the lattice Green function $D_{\alpha\beta} = \langle\langle X_f^\alpha | X_g^{-\beta}\rangle\rangle$ is just a Hubbard-I approximation for the intercluster hopping $T(\mathbf{k})$:

$$D^{-1}(\mathbf{k}, \omega) = (D^0(\omega))^{-1} - T(\mathbf{k}). \tag{4}$$

Here all functions are matrixes in α, β index, and

$$D^0_{\alpha\beta}(\omega) = \delta_{\alpha\beta} F(\alpha)/[\omega - \Omega(\alpha)], \tag{5}$$

$$\Omega(\alpha) = E_q(N+1) - E_p(N) - \mu, \tag{6}$$

$$F(\alpha) = \langle X^{pp}\rangle + \langle X^{qq}\rangle. \tag{7}$$

Here $D^0_{\alpha\beta}(\omega)$ is the exact cluster Green function. Its spectral weight may be zero when α describes the excitation between two empty states. Similar to the CDMFT+ED calculations [11, 13] our NC – CPT, as shown below in the Fig. 1, reproduces both poles and zeros of the electronic Green function

$$G_{\sigma\sigma'}(\mathbf{k}, \omega) = \frac{1}{N_c} \sum_{i,j=1}^{N_c} \sum_{\alpha\beta} \gamma_{i\sigma}(\alpha)\gamma^*_{j\sigma'}(\beta) \times \\ \times D_{\alpha\beta}(\mathbf{k}, \omega) e^{-i(\mathbf{r}_i - \mathbf{r}_j)\mathbf{k}}, \tag{8}$$

where N_c is the number of sites in the cluster (in our case is 4); i, j are site indexes in the cluster.

Doping results the redistribution of the spectral weight and change the band structure. For three different concentrations we plot in Fig. 1 the poles and zeros (left column) and map of the spectral weight $A(\mathbf{k}, \varepsilon_F)$ (momentum distribution curves or MDC in ARPES). The spectral weight

$$A(\mathbf{k}, \omega) = -\frac{1}{\pi} \operatorname{Im} G(\mathbf{k}, \omega + i\delta) \tag{9}$$

depends on the broadening δ. The central and right columns in Fig. 1 correspond to the different values of δ. The model parameters are

$$U/t = 4.3,\ t'/t = -0.13,\ t''/t = 0.16,$$

$$\delta/t = 0.01\ (\text{Fig. 1b, e, h}),\ \delta/t = 0.1\ (\text{Fig. 1c, f, i}).$$

The energy windows around Fermi level for spectral weight map was $\pm 0.2t$ for $\delta/t = 0.1$ and $\pm 0.02t$ for $\delta/t = 0.01$.

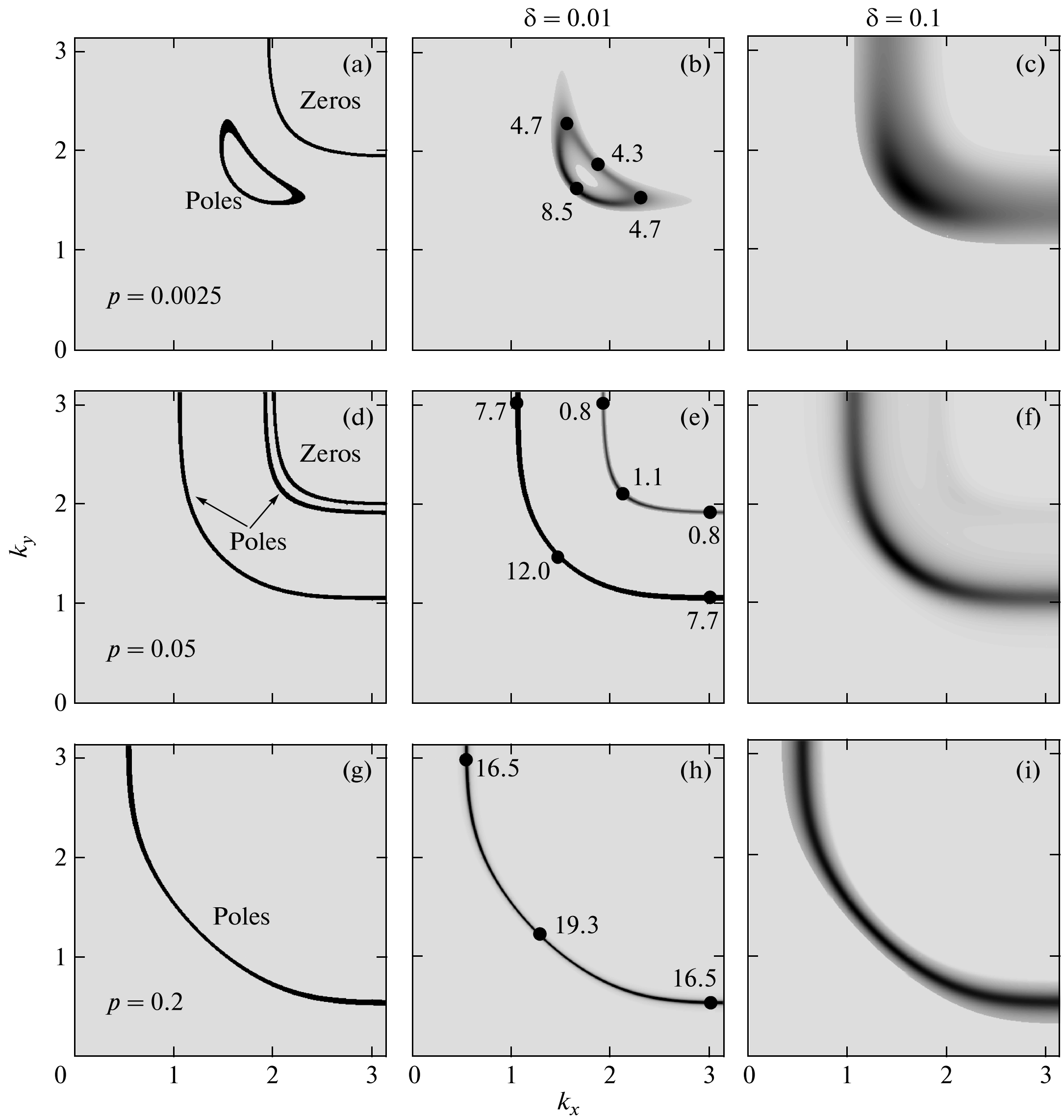

Fig. 1. Fermi surface in three different concentration regions: from poles and zeros of the Green-function (a) and spectral weight map with high resolution (b) and low resolution (c) for doping value $p = 0.0025$. The same in (d, e, f) for $p = 0.05$ and (g, h, i) for $p = 0.20$. The numbers at the different k points in (b, e, h) show the spectral weight in this point

The tight-binding fitting reproduce the ARPES data for optimal doping rather well (for example, for LSCO and Bi-2212). The nearest neighbor hopping integral found by this fitting $t \approx 0.25-0.4$ eV [21–23]. During last 10–15 years the typical energy resolution for ARPES was 10–45 meV [23–26]. Therefore, authors of many theoretical works take the broadening parameter to be $0.02-0.15t$ [12–15]. For instance, Fermi arc has been measured by ARPES in LSCO [23] with resolution $\delta = 0.02$ eV. The value of hopping parameter fitted the Fermi surface in that paper is $t = 0.25$ eV, thus we estimate the ratio $\delta/t = 0.08$. However, in the present days there is the laser-excited ARPES with the energy resolution about 1 meV [27].

At small doping the Fermi surface shows a small pocket (Fig. 1a). In the limit of small broadening the MDC gives also the same pocket. We have calculated it with different $\delta = 0.01t$ and $\delta = 0.1t$ (Fig. 1b, c). Nevertheless, the spectral weight varies along the pocket decreasing close to the line of zeros similar to the paper [11]. The resolution value $\delta = 0.1t$ results a transformation of the pocket into the arc (Fig. 1c) (similar transformation is obtained in the paper [13] for $\delta = 0.05t$). This transformation has been discussed by many authors before as mentioned in the review [3]. In the intermediate region $p_{c1} < p < p_{c2}$ the two Fermi surface and line of zeros around (π, π) are shown in Fig. 1d. The MDC reveals for small δ in Fig. 1e that the larger hole surface has also the order of magnitude large spectral weight than small electron surface. The MDC for $\delta = 0.1t$ (Fig. 1f) shows only one large hole Fermi surface while electron surface disappeared. Its spectral weight becomes too small. Finally at large doping both the poles (Fig. 1g) and MDC (Fig. 1h, i) show the same Fermi surface independently of the broadening value.

The concentration dependence of the spectral weight for $\delta = 0.1t$ is shown in Fig. 2. The suppression of the

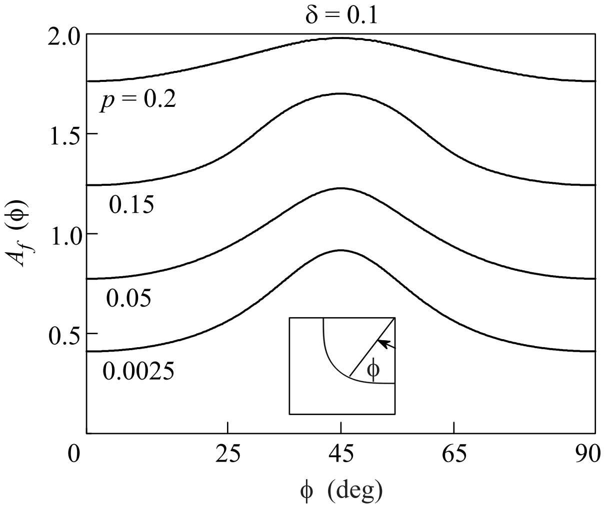

Fig. 2. Angle dependence of the spectral weight along the Fermi surface for different doping values and broadening $\delta = 0.1t$

spectral weight in the antinodal point related to the pseudogap is maximal at small doping and gradually decreases with increasing doping. This behavior corresponds well to the ARPES data [1].

In conclusion, we have shown that the concentration dependence of the true Fermi surface (left column in Fig. 1) and MDC with low resolution (right column in Fig. 1) gives different results. While the Fermi surface has three different types of topology separated by two Lifshitz transitions the ARPES gives the arc with smoothly increasing length. Only order of magnitude improvement in energy resolution will allow to obtain the true Fermi surface by MDC as shown in the central column in Fig. 1.

This work is supported by Presidium RAS Program 18.7, RFBR (Grants # 09-02-00127, # 10-02-90725-mob_st), Integration Project SBRAS N40, and FCP Program “Kadry” Goskontract P891.

1. A. Damascelli, Z. Hussein, and Z. X. Shen, Rev. Mod. Phys. **75**, 473 (2003).
2. N. Doiron-Leyrand, C. Proust, D. LeBoeuf et al., Nature **447**, 565 (2007).
3. M. R. Norman, Physics **3**, 86 (2010).
4. S. G. Ovchinnikov, E. I. Shneyder, and M. M. Korshunov, J. Phys.: Condens Matter **23**, 045701 (2011).
5. S. V. Nikolaev and S. G. Ovchinnikov, Zh.Exp.Teor.Fiz. **138**, 717 (2010) [J. Exp. Theor. Phys. **111**, 634 (2010)].
6. A. F. Barabanov, A. A. Kovalev, O. V. Urazaev et al., Zh. Exp. Teor. Fiz. **119**, 777 (2001) [J. Exp. Theor. Phys. **92**, 677 (2001)].
7. S. G. Ovchinnikov and M. M. Korshunov, Eur. Phys. J. B **57**, 271 (2007).
8. N. M. Plakida and V. S. Oudovenko, Zh. Exp. Teor. Fiz. **131**, 259 (2007) [J. Exp. Theor. Phys. **104**, 230 (2007)].
9. L. Hosoi, M. S. Laad, and P. Fulde, Phys. Rev. B **78**, 165107 (2008).
10. S. Chakravarty and H.-Y. Kee, Proc. Nat. Acad. Sc. (USA) **105**, 8835 (2008).
11. T. D. Stanescu and G. Kotliar, Phys. Rev. B **74**, 125110 (2006).
12. B. Kyung, S. S. Kancharla, D. Senechal et al., Phys. Rev. B **73**, 165114 (2006).
13. S. Sakai, Y. Motome, and M. Imada, Phys. Rev. Lett. **102**, 056404 (2009).
14. A. Liebsh and N.-H. Tong, Phys. Rev. B **80**, 165126 (2009).
15. M. Civelli, Phys. Rev. B **79**, 195113 (2009).
16. M. Potthoff, Eur. Phys. J. B **32**, 429 (2003).
17. T. Maier, M. Jarrell, T. Pruschke, and M. Hettler, Rev. Mod. Phys. **77**, 1027 (2005).
18. G. Kotliar, S. Y. Savrasov, K. Haule and et al., Rev. Mod. Phys. **78**, 865 (2006).
19. D. Senechal, D. Perez, and M. Pioro-Ladriere, Phys. Rev. Lett. **84**, 522 (2000).
20. R. O. Zaitzev, Zh. Exp.Teor. Fiz. **70**, 1100 (1976) [J. Exp. Theor. Phys. **43**, 574 (1976)].
21. A. A. Kordyuk, S. V. Borisenko, M. Knupfer, and J. Fink, Phys. Rev. B **67**, 064504 (2003).
22. W. Prestel, F. Venturini, B. Muschler et al., Eur. Phys. J. ST**188**, 163 (2010).
23. T. Yoshida, X. J. Zhou, D. H. Lu et al., Condens Matter **19**, 125209 (2007).
24. D. S. Marshall, D. S. Dessau, A. G. Loeser et al., Phys. Rev. Lett. **76**, 4841 (1996).
25. A. Ino, C. Kim, M. Nakamura et al., Phys. Rev. B **62**, 4137 (2000).
26. T. Yoshida, M. Hashimoto, T. Takizawa et al., Phys. Rev. B **82**, 085119 (2010).
27. K. Ishizaka, T. Kiss, S. Izumi et al., Phys. Rev. B **77**, 064522 (2008).